nature medicine

Dynamic regulation of cardiolipin by the lipid pump Atp8b1 determines the severity of lung injury in experimental pneumonia

Nancy B Ray[1,8], Lakshmi Durairaj[1,8], Bill B Chen[2], Bryan J McVerry[2], Alan J Ryan[1], Michael Donahoe[2], Alisa K Waltenbaugh[2], Christopher P O'Donnell[2], Florita C Henderson[1], Christopher A Etscheidt[1], Diann M McCoy[1], Marianna Agassandian[1], Emily C Hayes-Rowan[2], Tiffany A Coon[2], Phillip L Butler[3], Lokesh Gakhar[3], Satya N Mathur[1], Jessica C Sieren[1], Yulia Y Tyurina[4], Valerian E Kagan[4], Geoffrey McLennan[1,5,6] & Rama K Mallampalli[2,7]

Pneumonia remains the leading cause of death from infection in the US, yet fundamentally new conceptual models underlying its pathogenesis have not emerged. We show that humans and mice with bacterial pneumonia have markedly elevated amounts of cardiolipin, a rare, mitochondrial-specific phospholipid, in lung fluid and find that it potently disrupts surfactant function. Intratracheal cardiolipin administration in mice recapitulates the clinical phenotype of pneumonia, including impaired lung mechanics, modulation of cell survival and cytokine networks and lung consolidation. We have identified and characterized the activity of a unique cardiolipin transporter, the P-type ATPase transmembrane lipid pump Atp8b1, a mutant version of which is associated with severe pneumonia in humans and mice. Atp8b1 bound and internalized cardiolipin from extracellular fluid via a basic residue–enriched motif. Administration of a peptide encompassing the cardiolipin binding motif or *Atp8b1* gene transfer in mice lessened bacteria-induced lung injury and improved survival. The results unveil a new paradigm whereby Atp8b1 is a cardiolipin importer whose capacity to remove cardiolipin from lung fluid is exceeded during inflammation or when Atp8b1 is defective. This discovery opens the door for new therapeutic strategies directed at modulating the abundance or molecular interactions of cardiolipin in pneumonia.

Pneumonia can be a devastating and immediate cause of death among all age groups, and it is second only to childbirth for hospital admission[1]. Thus, it remains a major cause of morbidity and contributes substantially to healthcare costs in both the community and among hospitalized individuals. The pathobiology of bacterial pneumonia after infection with highly virulent pathogens (*Streptococcus pneumoniae*, *Staphylococcus aureus*, *Haemophilus influenzae* and *Escherichia coli*) typically involves neutrophilic lung infiltration and a robust host immune response, leading to severe ventilatory abnormalities. Numerous microbial virulence and host factors participate in the progression of pulmonary injury[2]. Yet despite decades of intensive study, there has been a lack of fundamentally new biological mechanisms with regard to the pathobiology of bacterial pneumonia. Consequently, there has been an overreliance on the use of broad-spectrum antibiotics in severe infection, causing the emergence of multidrug-resistant bacterial strains.

Cardiolipin is typically a minor component of pulmonary lavage fluid and comprises only ~1–2% of alveolar surfactant, a surface tension–lowering material enriched with phosphatidylcholine and key apoproteins that is secreted into the airways by type II alveolar epithelia[3]. High amounts of cardiolipin are seen in lung injury models, and cardiolipin is enriched in mitochondrial and some bacterial membranes[4–6]. However, the biological role and mechanisms for changes in cardiolipin content during inflammatory injury remain enigmatic. The findings of very low cardiolipin concentrations in lung fluid under healthy conditions suggest the existence of control mechanisms that tightly regulate cardiolipin availability within the airways or extracellular fluid.

One population at increased risk for pneumonia includes individuals with progressive familial intrahepatic cholestasis type 1 (PFIC1, or Byler's disease)[7,8]. Pneumonia and respiratory symptoms have been seen in 13% and 26% of people with PFIC1 (refs. 7,9). These individuals have mutations in ATP8b1. Type 4 P-type ATPases maintain lipid balance by translocating phospholipids from the outer to the inner leaflets of membrane bilayers. ATP8b1 translocates phosphatidylserine from the outer to the inner membrane in cells, is highly expressed in

[1]Department of Internal Medicine, University of Iowa, Iowa City, Iowa, USA. [2]Department of Internal Medicine, Acute Lung Injury Center of Excellence, University of Pittsburgh, Pittsburgh, Pennsylvania, USA. [3]Department of Biochemistry, University of Iowa, Iowa City, Iowa, USA. [4]Center for Free Radical and Antioxidant Health, Department of Environmental and Occupational Health, University of Pittsburgh, Pittsburgh, Pennsylvania, USA. [5]Department of Radiology, University of Iowa, Iowa City, Iowa, USA. [6]Department of Biomedical Engineering, University of Iowa, Iowa City, Iowa, USA. [7]Medical Specialty Service Line, Veteran's Affairs Pittsburgh Healthcare System, Pittsburgh, Pennsylvania, USA. [8]These authors contributed equally to this work. Correspondence should be addressed to R.K.M. (mallampallirk@upmc.edu).

Received 11 June; accepted 17 August; published online 19 September 2010; doi:10.1038/nm.2213

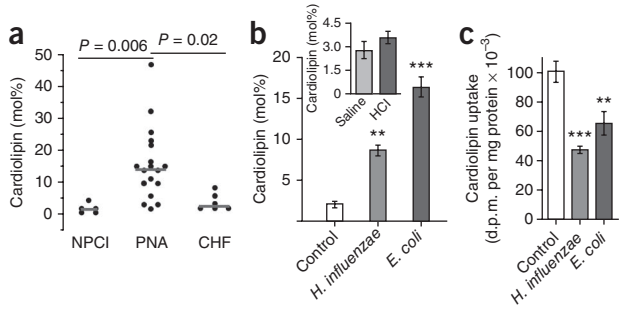

Figure 1 Quantification of cardiolipin in subjects with pneumonia. (**a**) Median (gray line) and distribution (black circles) of cardiolipin abundance in tracheal aspirates from subjects with nonpulmonary critical illness (NPCI, $n = 5$), pneumonia (PNA, $n = 17$) and CHF ($n = 6$). (**b**) Quantification of cardiolipin in mice with pneumonia. C57BL/6 mice were infected i.t. with *E. coli* (1×10^6 CFU per mouse, $n = 4$), *H. influenzae* (2×10^8 CFU per mouse, $n = 5$) or left uninfected ($n = 3$). Mice were killed 48 h (*E. coli*) or 72 h (*H. influenzae*) later and their lungs were lavaged and processed for cardiolipin determination. Inset, cardiolipin concentrations after acid instillation. Mice (six per group) were given HCl (pH 1.5, 2 ml per kg body weight i.t.) before being killed 30 min later for analysis of BAL cardiolipin abundance. (**c**) Cellular cardiolipin uptake in primary type II lung epithelia. Cells (from $n = 10$ mice) were cultured with [^{3}H]cardiolipin for 2 h at 37 °C in the presence or absence of *E. coli* (multiplicity of infection = 100) or *H. influenzae* (multiplicity of infection = 10). Data are quantified as disintegrations per minute (d.p.m.). In **b** and **c**, ** $P < 0.01$ and *** $P < 0.001$ versus control (means ± s.d.), as determined by one-way analysis of variance (ANOVA).

apical epithelial membranes and is present in various human tissues[8]. The observation that people with PFIC1 are prone to respiratory infection, coupled with the ability of ATP8b1 to transport phospholipids across cellular membranes, led us to hypothesize that ATP8b1 is a cardiolipin import protein. To test this hypothesis, we analyzed Atp8b1-defective mice that harbor a naturally occurring ATP8b1 mutation (G308V) observed in individuals with severe PFIC1.

In this study, we discovered that cardiolipin concentrations are elevated in the lung fluid of individuals with pneumonia and that it is a highly potent surfactant inhibitor that disrupts lung structure and function. The abundance of cardiolipin in lung fluid is regulated by Atp8b1, which effectively binds and internalizes cardiolipin in lung epithelia via domain-specific interactions. Atp8b1-mutant mice have elevated cardiolipin concentrations in lung fluid and are prone to bacterial-induced lung injury. These results provide a new conceptual model for bacterial pneumonia, where Atp8b1 serves as a molecular transporter that removes an injurious bioactive lipid from distal airways to preserve pulmonary function.

RESULTS

Cardiolipin is elevated in pneumonitis

We quantified cardiolipin in tracheal aspirates from critically ill subjects with nonpulmonary illnesses ($n = 5$), clinically diagnosed pneumonia ($n = 17$) or congestive heart failure (CHF) ($n = 6$) (**Supplementary Table 1**). The control subjects with nonpulmonary illnesses included some requiring mechanical ventilation for liver failure, and some with hemolysis elevated liver enzymes low platelets (HELLP) syndrome, Guillain-Barré syndrome, renal failure or gastrointestinal tract bleeding. Subjects with pneumonia were identified as having new or changing radiographic pulmonary infiltrates, increasing sputum quantity or change in sputum character, and clinical features such as fever, elevated white blood cell count and hypoxemia, without dependence upon sputum culture results or distinction between community or hospital acquisition (data not shown). No bacterial growth was detected in 39% (7/17) of tracheal aspirates from subjects with pneumonia, whereas *S. pneumoniae* grew from four subjects, *Pseudomonas aeruginosa* and *S. aureus* grew from three subjects each and *H. influenzae* grew from one subject. Ninety percent (26/28) of all subjects were on broad-spectrum antibiotics on the day of tracheal aspirate collection (**Supplementary Table 1**). Subjects with pneumonia had significantly higher amounts of cardiolipin (median = 12.9 mol%) in tracheal aspirates compared to subjects with nonpulmonary diagnoses (~9.7 fold) or CHF (approximately sixfold, Kruskal-Wallis $P = 0.0007$, **Fig. 1a**). Notably, cardiolipin abundance did not correlate with culture status, bacterial pathogen, duration of mechanical ventilation, gender or age (**Supplementary Fig. 1**).

We also infected mice with strains of *H. influenzae* or *E. coli* that cause pneumonia[10,11]. Bronchoalveolar lavage (BAL) fluid from infected mice had greater amounts of cardiolipin than BAL isolated from uninfected mice (**Fig. 1b**). To assess whether the high cardiolipin levels were due to reduced cellular uptake, we cultured primary mouse type II lung epithelia with [^{3}H]cardiolipin. Infection of cells with *H. influenzae* or *E. coli* resulted in significantly less cellular uptake of [^{3}H]cardiolipin (**Fig. 1c**). Thus, cardiolipin concentrations are increased in lung fluid of both humans and mice with pneumonitis, and this may be the result of decreased epithelial uptake of the phospholipid.

Because cardiolipin is a constituent of bacterial membranes, it is plausible that its release into lung fluid during pneumonia represents infections having very high bacterial burdens. Alternatively, elevated cardiolipin in lung fluid could originate from dying host cells, as it is exclusively present within the inner mitochondrial membrane and is released during intrinsic mitochondria-dependent apoptosis. Because the molecular signatures of cardiolipin species differ between mammalian cells and bacterial membranes, we examined the source of cardiolipin in humans with pneumonia (**Supplementary Fig. 2a**) and mice infected with *E. coli* (**Supplementary Fig. 2b**). Electrospray ionization mass spectrometry spectra of these cardiolipins obtained from human and mouse samples show that cardiolipin originates from mammalian cells. Thus, we found mitochondria-specific mammalian species of cardiolipin, and not bacterial types, in lung fluid samples.

Cardiolipin impairs lung structure, function and cell viability

We measured surface tension–lowering activity of lipid vesicles *in vitro*. The lipid vesicles were generated by incorporating phospholipids (cardiolipin, lysophosphatidylcholine and phosphatidylserine) into Infasurf, a commercial apoprotein-containing surfactant that lowers surface tension (**Fig. 2a**). We also extracted lipids from Infasurf by organic solvent extraction to generate Infasurf protein-deficient preparations that we reconstituted with phospholipids for testing (**Fig. 2b**). Unlike phosphatidylserine, cardiolipin at high concentrations (>3 mol%) resulted in increased surface tension (**Fig. 2a**). Cardiolipin impaired the surface tension–lowering activity of Infasurf to a greater extent than did lysophosphatidylcholine, a positive control (**Fig. 2a**)[12]. These adverse effects of cardiolipin were more pronounced when testing Infasurf extracts devoid of surfactant-associated apoproteins (**Fig. 2b**). Mice given intratracheal (i.t.) cardiolipin had significantly lower lung compliance and higher elastance and resistance compared to controls (**Fig. 2c–f**). Cardiolipin administration also increased BAL protein concentration (**Supplementary Fig. 3a**), differentially altered surfactant protein expression (**Supplementary Fig. 3b**) and reduced γ-interferon and interleukin-2 (IL-2) protein levels and increased

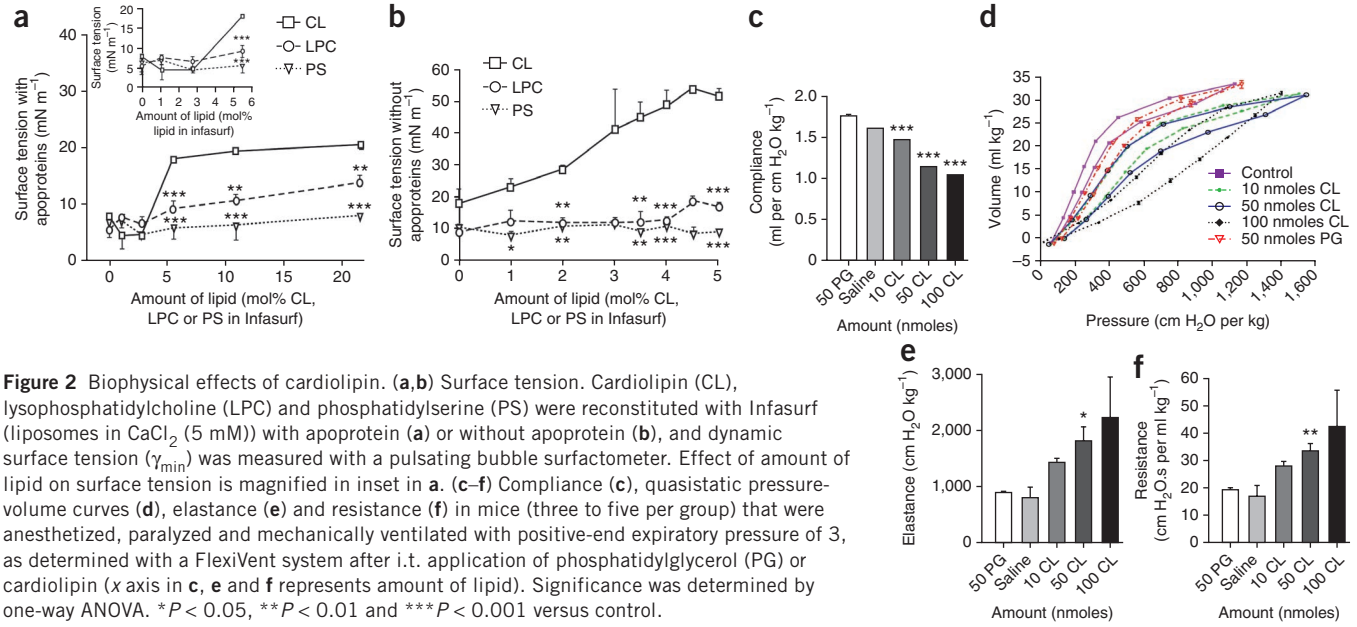

Figure 2 Biophysical effects of cardiolipin. (**a**,**b**) Surface tension. Cardiolipin (CL), lysophosphatidylcholine (LPC) and phosphatidylserine (PS) were reconstituted with Infasurf (liposomes in $CaCl_2$ (5 mM)) with apoprotein (**a**) or without apoprotein (**b**), and dynamic surface tension (γ_{min}) was measured with a pulsating bubble surfactometer. Effect of amount of lipid on surface tension is magnified in inset in **a**. (**c**–**f**) Compliance (**c**), quasistatic pressure-volume curves (**d**), elastance (**e**) and resistance (**f**) in mice (three to five per group) that were anesthetized, paralyzed and mechanically ventilated with positive-end expiratory pressure of 3, as determined with a FlexiVent system after i.t. application of phosphatidylglycerol (PG) or cardiolipin (*x* axis in **c**, **e** and **f** represents amount of lipid). Significance was determined by one-way ANOVA. $*P < 0.05$, $**P < 0.01$ and $***P < 0.001$ versus control.

IL-10 protein levels (**Supplementary Fig. 3c**,**d**), but it did not affect the distribution of various inflammatory cells (**Supplementary Fig. 3e**) in BAL. Thus, cardiolipin in lung fluid adversely affects lung mechanics by greatly impairing surfactant activity. It also modulates expression of cytokine networks that could affect lung function.

We next addressed whether the adverse functional effects of cardiolipin led to altered lung structure. Mice were subjected to live imaging of lungs by microcomputed tomography (microCT) scanning (**Supplementary Methods**). Compared to mice given diluent, mice given cardiolipin (50 nmol) had more prominent markings in parenchyma with scattered patchy areas of alveolar consolidation (**Fig. 3a**). These abnormalities were more severe after high doses of cardiolipin. Histological analysis identified areas of alveolar infiltration and the appearance of foamy cells within alveoli (**Fig. 3a**). High-dose cardiolipin produced edema and disruption of alveolar lining cells (**Fig. 3a**–**c**) that contributed to fatality of mice within 2–3 h. Cardiolipin activated the apoptotic program in cells and in tissue (**Fig. 3d**) and decreased cell viability (**Fig. 3e**,**f**).

Atp8b1 is an alveolar epithelial cardiolipin importer

Because cardiolipin is internalized by alveolar cells (**Fig. 1c**), we hypothesized that cells would express an import protein that regulates cardiolipin abundance in lung fluid. ATP8b1 was a candidate protein, as it internalizes phospholipids and because humans with ATP8b1 defects are prone to pneumonia[9]. Mouse type II cells had high level expression of Atp8b1 compared to macrophages or fibroblasts (**Supplementary Fig. 4a**), and this expression was upregulated by phospholipids (**Supplementary Fig. 4b**) and localized predominately to the cell surface (**Supplementary Fig. 4c**). Cells expressing lentivirus-encoded Atp8b1 had higher levels of mRNA and protein expression, coupled with a robust increase in the uptake of fluorescent nitrobenzoxadiazole (NBD)-labeled cardiolipin or phosphatidylserine (positive control) compared to untransduced cells (**Fig. 4a**,**b** and **Supplementary Fig. 4d**). Atp8b1-overexpressing cells had greater fluorescence on both the cell surface and inside the cells, indicating that the NBD-labeled cardiolipin was located on the plasma membrane and within the cytoplasm. Although Atp8b1 internalized cardiolipin, it did not enhance GFP-labeled *E. coli* uptake (**Supplementary Fig. 4e**). Notably, *H. influenzae* triggers Atp8b1 degradation and ubiquitination (**Supplementary Fig. 5**). Other related ATP-driven pumps, Atp8a1 and Atp11a, did not transport cardiolipin (**Supplementary Fig. 6**).

We also gave mice adenovirus (Ad5) encoding Atp8b1 or empty adenovirus intratracheally before *E. coli* infection to assess lung function. Mice infected with *E. coli* at 1×10^6 colony-forming units (CFU) per mouse had cleared the pathogens by 48 h of analysis (data not shown). These mice showed decreased percentages of BAL macrophages with a neutrophilic infiltrate typical of pneumonia, a profile not affected 72 h after Ad5-*Atp8b1* gene transfer (**Supplementary Fig. 7a**). Mice given Ad5 alone or Ad5 encoding Atp8b1 tended to have high BAL protein concentrations associated with the release of proinflammatory cytokines after bacterial infection (**Supplementary Fig. 7b**,**c**). *Atp8b1* gene delivery before *E. coli* infection also lowered the expression of collectins, surfactant protein A (SP-A) and SP-D but did not affect the expression of SP-B, the latter being essential for surfactant activity (**Supplementary Fig. 7d**). Notably, *Atp8b1* gene delivery effectively increased Atp8b1 levels, lowered cardiolipin levels and reversed *E. coli*–induced impairment of lung mechanics (**Fig. 4c**,**d** and **Supplementary Fig. 7e**) compared to infected mice given empty Ad5. *Atp8b1* gene transfer did not reduce apoptosis after bacterial infection (**Fig. 4e**). Thus, the primary mechanism for the beneficial effects of increased Atp8b1 expression is reduced cardiolipin availability, which preserves surfactant function and improves lung mechanics. These effects were sufficient to result in increased survival of *E. coli*–infected mice (**Fig. 4f**).

We performed additional loss-of-function studies with *Atp8b1*-specific siRNA and Atp8b1-mutant mice that harbor a single amino acid substitution (G308V) resulting in a defect in cellular import of phosphatidylserine[13,14]. *Atp8b1*-targeting siRNA produced a significant decrease in cardiolipin uptake and specifically reduced the amount of immunoreactive Atp8b1 compared to scrambled RNA (**Fig. 5a**). Restriction digests of genomic DNA revealed that the mutant mice lacked 500-bp and 300-bp digest fragments (**Fig. 5b**). We detected low-level Atp8b1 protein expression in mutant mouse liver and lung compared to wild-type mouse tissues (**Fig. 5c**). Atp8b1-mutant mice had significantly higher BAL cardiolipin concentrations as compared to wild-type littermates

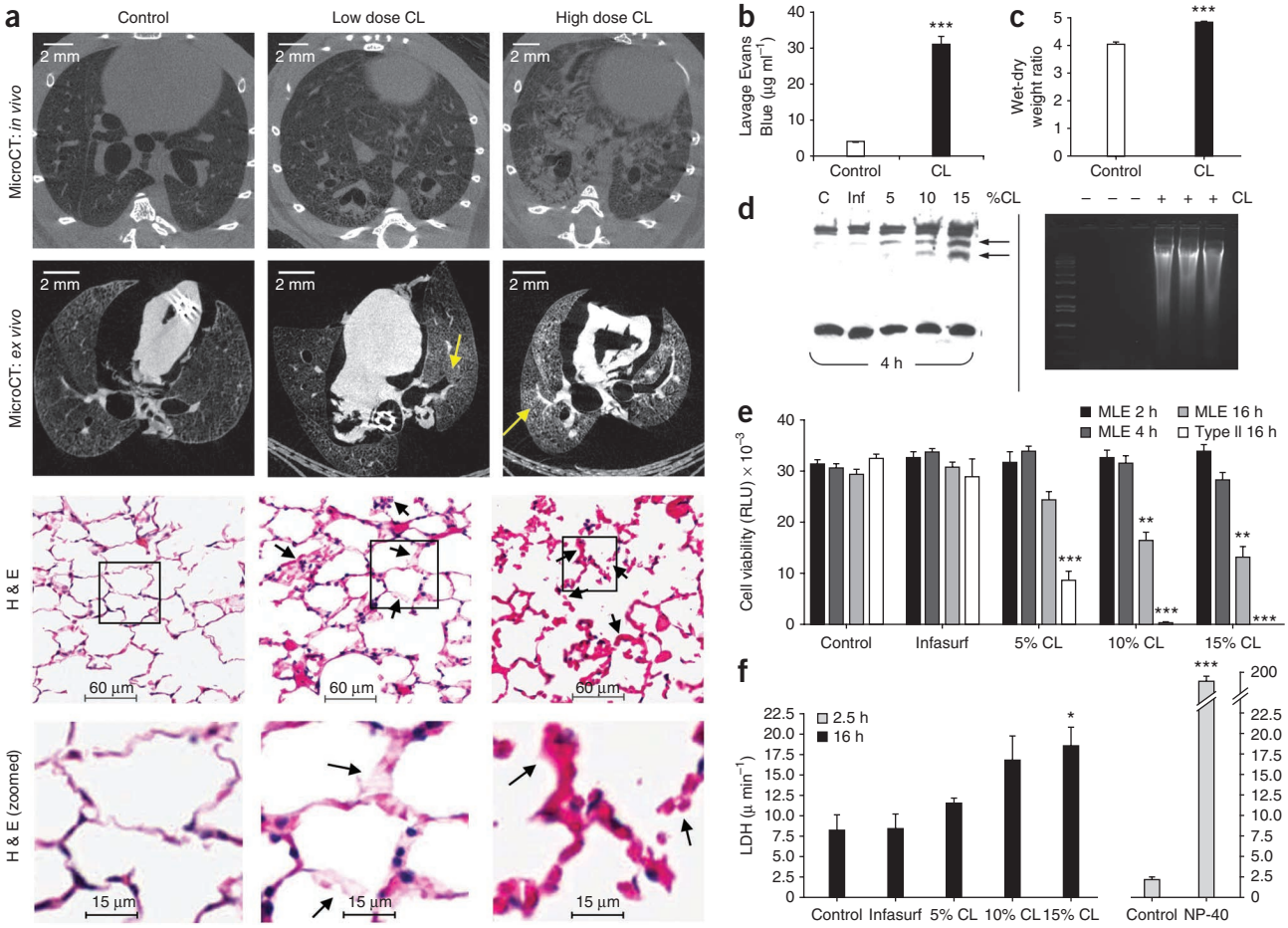

Figure 3 Effect of cardiolipin on lung structure and epithelial cell viability. (**a**) MicroCT scan images were obtained on live mice (*in vivo*) 1 h after i.t. administration of cardiolipin (50 nmol, (low), 100 nmol (high)) versus control mice (top images). In separate studies, mice were given cardiolipin as above, and their lungs were fixed and processed for microCT scanning (*ex vivo*). Images are representative of two mice per group. Fixed tissue was also processed for H & E staining, and the bottom images show a high magnification (100×) image of foamy cells. (**b**,**c**) Lung edema. Mice given cardiolipin (15 mM in 50 μl saline, i.t.; $n = 3$) or vehicle (50 μl saline; $n = 3$) were assessed for Evans Blue dye extravasation in lung fluid. Wet-dry weights of lungs were also determined (**c**). $^{***}P < 0.01$ versus control. (**d**) Apoptosis. Left, poly(ADP-ribose) polymerase (PARP) cleavage (arrows) as a marker of apoptosis in primary mouse type II cells exposed to Infasurf (120 nmol ml^{-1}) or cardiolipin (5–15 mol%). Right, analysis of lung DNA fragmentation in mice given i.t. cardiolipin (50 nmol). (**e**,**f**) Cell viability (**e**) or lactate dehydrogenase (LDH) release (**f**, primary type II cells) after cardiolipin exposure at 2 h, 2.5 h, 4 h and 16 h of lipid exposure. NP-40 was used as a positive control for LDH release. Data represent three separate experiments, where $^{*}P < 0.05$, $^{**}P < 0.01$ and $^{***}P < 0.001$ versus control, as determined by one-way ANOVA.

(**Fig. 5d**). Consistent with Atp8b1's inability to alter uptake of bacteria, bacterial loads did not differ between Atp8b1-mutant and wild-type mice (**Supplementary Fig. 8a**). Both Atp8b1-defective and wild-type littermates showed no differences in BAL protein content (**Supplementary Fig. 8b**), wet-dry lung weight ratios (**Supplementary Fig. 8c**) or cellular inflammation (**Supplementary Fig. 8d**) after *E. coli* infection. Of note, ATP8b1-defective mice had a blunted cytokine response to T helper type 1 cytokines (interferon (IFN)-γ, tumor necrosis factor (TNF)-α and IL-1β) compared to wild-type littermates after *E. coli* infection (**Supplementary Fig. 9a**,**b**) which may be secondary to increased expression of SP-A and SP-D (**Supplementary Fig. 9c**)[15,16]. Primary type II cells isolated from Atp8b1-mutant mice had significantly ($P < 0.05$) reduced NBD-cardiolipin uptake compared to cells isolated from wild-type littermates (**Fig. 5e**). Mutant mice also had impaired biophysical properties compared to wild-type mice, particularly after *E. coli* infection (**Fig. 5f**,**g** and **Supplementary Fig. 9d**). Although lung cells from mutant mice were more prone to apoptosis (**Fig. 5h**), there was no significant difference in mortality between Atp8b1-mutant and wild-type mice with infection (**Fig. 5i**). Collectively, these studies strongly suggest that Atp8b1 is a *bona fide* alveolar epithelial cardiolipin import pump.

Cardiolipin binding domain peptide blocks cardiolipin effects

We mapped the Atp8b1 cardiolipin binding domain (CBD). We synthesized deletion mutants by *in vitro* translation (**Supplementary Fig. 10a**,**b**) and then reacted them with 15 lipids prespotted onto hydrophobic lipid strips (**Supplementary Fig. 10c**). With this system, we found that full-length Atp8b1 and specific mutants bound cardiolipin and also sulfatide (sulfated galactosylceramides) (**Supplementary Fig. 10c**). C-terminal truncation mutants containing only the first 810 or 771 residues did not bind cardiolipin, suggesting that the CBD resides between residues 810 and 850 within Atp8b1. We confirmed this by testing a fragment (residues 771–850) that was sufficient for cardiolipin binding, indicating that a CBD resides within the Atp8b1 carboxy terminus (**Supplementary Fig. 10c**).

We expressed and purified GST fused to the putative CBD from cells. Mouse lung epithelial (MLE) cells cultured with GST-CBD peptide showed an 83% decrease in [^{3}H]cardiolipin uptake compared

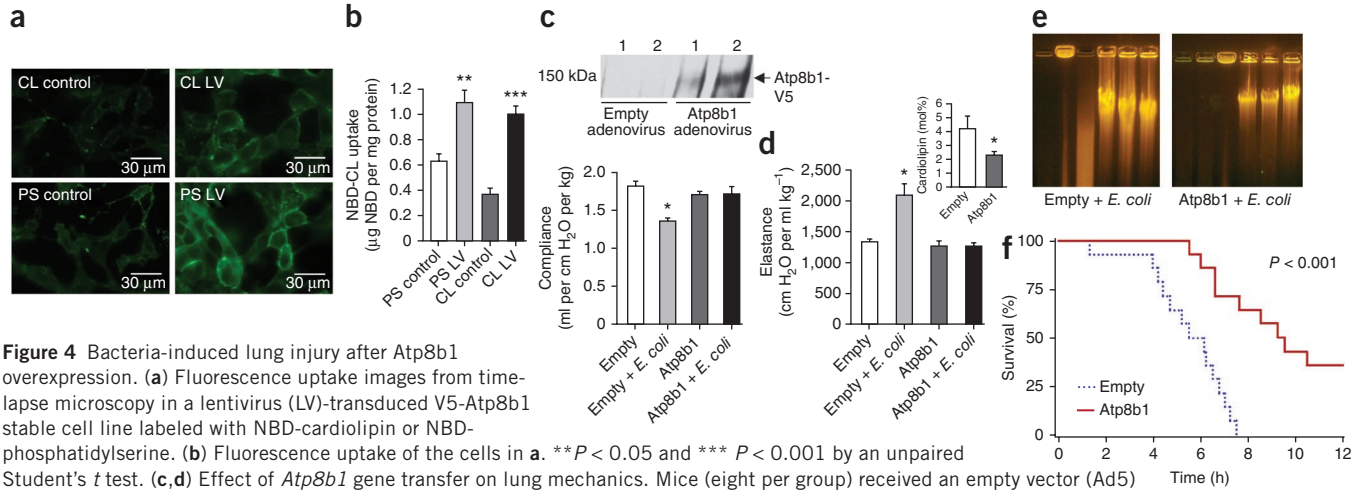

Figure 4 Bacteria-induced lung injury after Atp8b1 overexpression. (**a**) Fluorescence uptake images from time-lapse microscopy in a lentivirus (LV)-transduced V5-Atp8b1 stable cell line labeled with NBD-cardiolipin or NBD-phosphatidylserine. (**b**) Fluorescence uptake of the cells in **a**. $^{**}P < 0.05$ and $^{***}P < 0.001$ by an unpaired Student's *t* test. (**c**,**d**) Effect of *Atp8b1* gene transfer on lung mechanics. Mice (eight per group) received an empty vector (Ad5) or Ad5-Atp8b1 i.t. and 24 h later were given *E. coli* for 48 h before analysis of lung compliance (**c**, bottom) and elastance (**d**) determined as in **Figure 2**. (**c**) A representative immunoblot showing amounts of V5-immunoreactive Atp8b1 in lung tissue from two mice receiving Ad5 or Ad5-Atp8b1 (top). The inset in **d** shows cardiolipin concentrations in BAL fluid after Ad5-Atp8b1 or Ad5 infection. Significance was determined by a one-way ANOVA in **c** and **d**, where $^{*}P < 0.05$ for empty + *E. coli* versus other groups (means ± s.d.). (**e**) Lung DNA fragmentation in mice ($n = 6$) treated as in **c**. (**f**) Kaplan-Meier survival curve for mice infected with Ad5 empty or Ad5-Atp8b1 and infected with *E. coli* (5×10^6 CFU per mouse, $n = 14$ mice per group, $P < 0.001$, log-rank test).

to culture with GST peptide alone (**Fig. 6a**). Mice infected or not with *E. coli* and given intratracheal CBD peptide had a trend toward increased proportion of macrophages and modestly reduced protein content and neutrophils in BAL as compared to mice given vehicle (**Supplementary Fig. 11a,b**). Notably, CBD peptide profoundly lowered TNF-α and IL-1β protein levels and significantly ($P < 0.05$) reduced granulocyte-macrophage colony–stimulating factor protein amounts in BAL after bacterial infection (**Fig. 6** and **Supplementary Fig. 11c**). Cardiolipin also inhibited key cell survival pathways, an effect blocked by CBD peptide (**Supplementary Fig. 12**). CBD

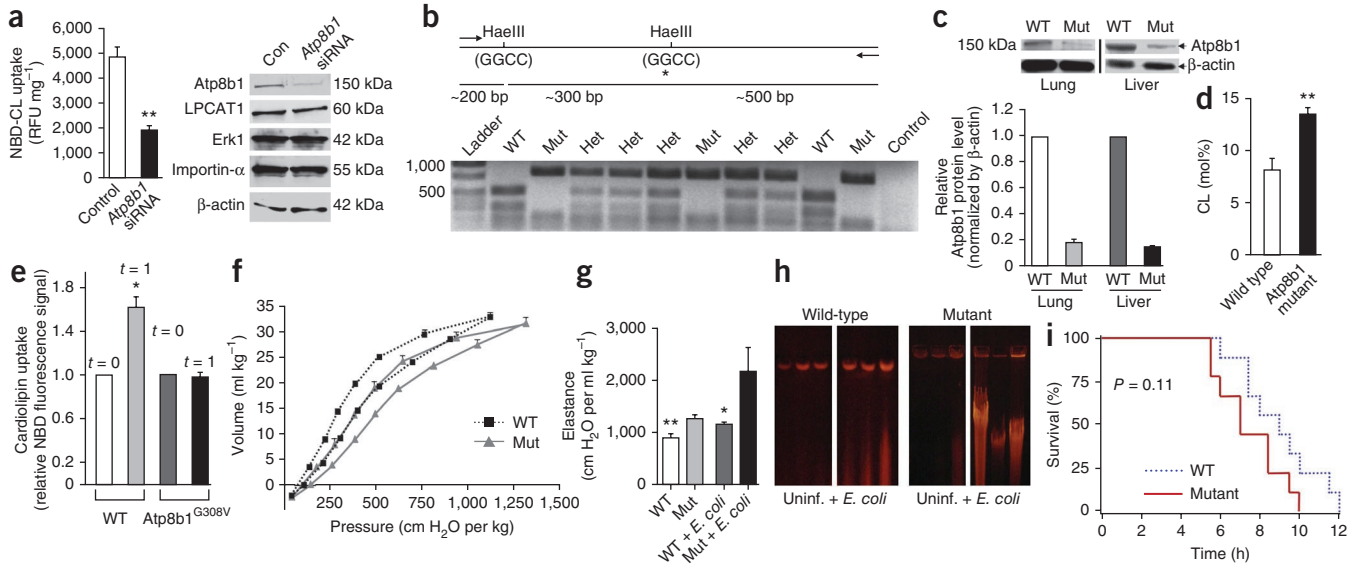

Figure 5 Bacteria-induced lung injury in Atp8b1-mutant mice. (**a**) NBD-labeled cardiolipin uptake (left) is quantified in human A549 alveolar type II (ATII)-like cells transfected with *Atp8b1*-specific siRNA or control RNA. Immunoblotting (right) with 25 μg of protein loaded per lane using cell lysates from siRNA studies. Blots were probed with antibodies specific for Atp8b1, lysophosphatidylcholine acyltransferase-1 (LPCAT1), extracellular signal–regulated kinase-1 (Erk1), importin-α and β-actin (used as specificity controls). $^{**}P < 0.01$. (**b**) HaeIII restriction digest patterns of genomic DNA used for genotyping wild-type (WT), heterozygous (Het) and mutant (Mut) mice. *Atp8b1*$^{G308V/G308V}$ mutant genomic DNA has a HaeIII restriction site (GGCC) in which the second G is mutated to T (glycine to valine) and is not recognized in restriction digests. (**c**) Top, Atp8b1 immunoblotting in mouse tissues. Bottom, densitometric analysis from six mice per group. (**d**) Cardiolipin concentrations in lung lavage from Atp8b1-mutant and wild-type littermates (three per group). $^{**}P < 0.01$. (**e**) NBD-cardiolipin uptake in primary type II epithelia isolated from mutants or wild-type littermates (five mice per group). Shown is NBD-cardiolipin cellular uptake initially after labeling ($t = 0$) and after 1 min. $^{*}P < 0.05$ versus other groups. (**f**,**g**) Lung mechanics in Atp8b1-mutant mice. Mutants and wild-type littermates uninfected or infected (seven per group) with *E. coli* were analyzed for determination of quasistatic volume-pressure curves (**f**, (uninfected)) and elastance (**g**). Statistical significance was determined by a one-way ANOVA in **g**. $^{**}P < 0.01$ WT versus Mut + *E. coli*, and $^{*}P < 0.05$ WT + *E. coli* versus Mut + *E. coli*. (**h**) Lung DNA fragmentation in wild-type and mutant mice (three per group) treated as in **g**. (**i**) Kaplan-Meier survival curve for wild-type and Atp8b1-mutant mice infected with *E. coli* (5×10^6 CFU per mouse, seven mice per group, $P = 0.11$, log-rank test). Data shown as means ± s.d.

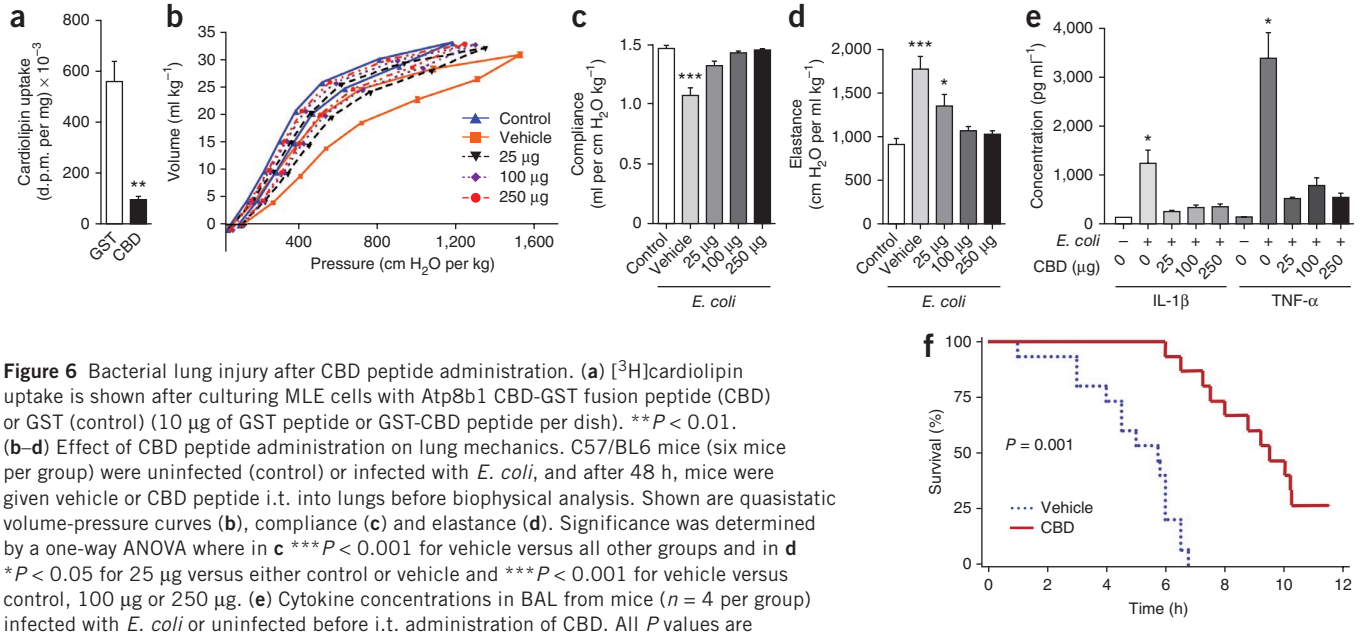

Figure 6 Bacterial lung injury after CBD peptide administration. (**a**) [^{3}H]cardiolipin uptake is shown after culturing MLE cells with Atp8b1 CBD-GST fusion peptide (CBD) or GST (control) (10 μg of GST peptide or GST-CBD peptide per dish). $^{**}P < 0.01$. (**b**–**d**) Effect of CBD peptide administration on lung mechanics. C57/BL6 mice (six mice per group) were uninfected (control) or infected with *E. coli*, and after 48 h, mice were given vehicle or CBD peptide i.t. into lungs before biophysical analysis. Shown are quasistatic volume-pressure curves (**b**), compliance (**c**) and elastance (**d**). Significance was determined by a one-way ANOVA where in **c** $^{***}P < 0.001$ for vehicle versus all other groups and in **d** $^{*}P < 0.05$ for 25 μg versus either control or vehicle and $^{***}P < 0.001$ for vehicle versus control, 100 μg or 250 μg. (**e**) Cytokine concentrations in BAL from mice ($n = 4$ per group) infected with *E. coli* or uninfected before i.t. administration of CBD. All *P* values are <0.05 for vehicle buffer + *E. coli*. (0+) versus other groups. (**f**) Kaplan-Meier survival curve for mice given i.t. CBD peptide (100 μg) and infected with *E. coli* (5×10^6 CFU per mouse, $n = 14$ mice per group, $P = 0.001$, log-rank test). Data shown is means ± s.d.

peptide did not alter surfactant apoprotein content nor the degree of lung cell apoptosis (**Supplementary Fig. 13a,c**). Infected mice given vehicle had impaired lung mechanics, effects that were reversed after CBD peptide administration (**Fig. 6b–d** and **Supplementary Fig. 13b**). These beneficial effects of CBD peptide on pulmonary homeostasis led to significantly improved survival in mice (**Fig. 6f**). Thus, the CBD within Atp8b1 is functional with regard to substrate binding, and this peptide exerts biological effects in concert with its activity in antagonizing actions of cardiolipin *in vivo*.

DISCUSSION

Pneumonia remains a major public health challenge and a leading cause of intensive care unit admission. Antimicrobial agents are the cornerstone of therapy for bacterial pneumonia, but few nonantibiotic therapies have emerged that affect the outcomes of patients with severe infection. The data here provide a new conceptual model involving cardiolipin, imported by ATP8b1, that contributes to the pathobiology of pneumonia. We show that cardiolipin concentrations in pulmonary fluid are markedly elevated both in humans with pneumonia and in mice infected with bacterial pathogens. Cardiolipin potently impairs lung mechanics by antagonizing surfactant function, leading to high surface-tension pulmonary edema[17,18]. We also observed that cardiolipin disrupts pulmonary architecture and reduces epithelial cell viability. Our finding that the adverse effects of cardiolipin are antagonized by cardiolipin-binding peptide suggest that future studies might entail the use of small-molecule modifiers that regulate cardiolipin availability as new nonantibiotic treatment strategies for patients with pneumonia.

Cardiolipin, an apoptotic cell surface marker, could be released in lung fluid in pneumonia from either dying lung cells or from bacterial membranes. The cardiolipin content in some bacterial envelopes, such as that of *E. coli*, is very high, but it is undetectable in *H. influenzae* membranes[6,19]. Yet, as shown here, both pathogens reduced cardiolipin uptake and increased cardiolipin lung concentrations, suggesting other mechanisms for its origin. Early in programmed cell death, cardiolipin transmigrates to the outer mitochondrial membrane[20] and can also reach the outer leaflet of the cell's plasma membrane[21], where it may be readily integrated into surfactant. Although our analysis identified that cardiolipin originates from mammalian cells, the results do not totally exclude a bacterial origin, as amounts of bacterial cardiolipin in fluid could be transient, or prokaryotic organisms might use host cell mitochondrial cardiolipin that is incorporated into bacterial membranes.

We show that cardiolipin is profoundly effective in inhibiting surfactant activity; it was twice as potent as lysophosphatidylcholine, a gold standard reference[22]. Optimal surfactant activity depends on tight molecular packing of the major surfactant phospholipid, dipalmitoylphosphatidylcholine (DPPC), within a film at the air-surface interface. Cardiolipin's ability to block surface tension lowering by DPPC would be predicted because of its bulky molecular structure, which would impede DPPC packing. It is difficult to equate cardiolipin concentrations in human tracheal aspirates (**Fig. 1a**) with pathophysiologic amounts of cardiolipin incorporated into the DPPC film in human BAL fluid. This is because of considerable issues of recovery and sample dilution and tight binding of cardiolipin with mitochondrial proteins, hindering its extraction[23]. However, we observed inhibitory actions of cardiolipin even at very low concentrations (~2 mol%) when we used cardiolipin liposomes devoid of surfactant apoproteins. Thus, surfactant proteins may protect against cardiolipin inhibition, and adverse cardiolipin effects may be more pronounced when surfactant proteins are depleted[24]. When we added cardiolipin to liposomes with apoproteins, surface tension was markedly elevated. In this case, higher concentrations of cardiolipin (at 5–20 mol%), as seen in people with pneumonia, are needed to impair surface activity. The *in vitro* data suggest that cardiolipin concentrations that impair surface activity are within the pathophysiological range. These human observations need to be confirmed in larger studies adjusted for possible confounding factors (smoking status, illness severity, lung compliance and comorbidities), as the current results in tracheal aspirates are associative and lack measures such as cell counts and

proteins and were not adjusted for dilution. The use of bronchoscopy with BAL may further strengthen these associations by improving the accuracy of pneumonia diagnosis and adjusting for inflammatory markers. Subgroup analyses (for example, alveolar hemorrhage and stages of acute lung injury) are also essential in understanding these associations. Serial measurements during mechanical ventilation may better link tracheal colonization and resolving inflammation with cardiolipin content in tracheal aspirates.

Typically, very low cardiolipin concentrations are seen in human lavage fluid, suggesting that alveolar cells harbor active lipid transport mechanisms[25,26]. We have the following evidence in support of Atp8b1 as an authentic cardiolipin import protein: Atp8b1 binds cardiolipin within a highly charged inter-transmembrane domain loop, *in vivo* administration of a peptide containing this putative CBD signature or Ad5-*Atp8b1* gene transfer lowers cardiolipin levels, coupled with reduced lung injury severity, and Atp8b1-defective mice have increased cardiolipin levels and are vulnerable to bacterial-induced lung injury. The data might suggest that cardiolipin released during pulmonary infection exceeds the substrate binding capacity of Atp8b1. In such a scenario, bacteria could degrade Atp8b1 protein (**Supplementary Fig. 5**), mask the cardiolipin-binding pocket by inducing Atp8b1 conformational changes or reduce pump catalytic function. Presumably, redundant mechanisms for cardiolipin import are insufficient, as ATP8b1-mutant mice showed sensitivity to pulmonary sepsis.

To our knowledge, these studies are the first demonstrating cellular uptake of cardiolipin via protein binding. We mapped the ATP8b1 CBD to a 40-residue motif within a predicted intertransmembrane loop[27,28]. This loop contains several regulatory elements, including a D554N missense mutation seen in individuals with PFIC1 (ref. 27). As individuals with PFIC1 have a higher incidence of respiratory symptoms, there may be additional polymorphisms within the CBD that predispose affected individuals to infection. Administration of CBD peptide in mice substantially lessened pulmonary impairment after infection, suggesting that the molecular interactions between the ATP8b1 motif and cardiolipin are preserved *in vivo*. Manipulation of cardiolipin seems to modulate the inflammatory response and cell survival pathways, effects that are mitigated by CBD peptide. Thus, alveolar cardiolipin and the CBD peptide seem to exert immunomodulatory actions that could affect resolution of pulmonary injury. These results may eventually serve as a springboard to generate drug therapies to sequester or enhance clearance of injurious cardiolipin in pneumonia.

METHODS

Methods and any associated references are available in the online version of the paper at http://www.nature.com/naturemedicine/.

Note: Supplementary information is available on the Nature Medicine website.

ACKNOWLEDGMENTS

We thank M.E. Anderson, M.J. Welsh, J. Zabner and M. Gladwin for critical review of the manuscript and helpful suggestions. The *Atp8b1*$^{G308V/G308V}$ 129S1/SvlmJ mutant mice[14] were a generous gift from L. Bull (University of California–San Francisco). Nontypable *H. influenza* strain 12 bacteria were kindly provided by D. Look (University of Iowa)[29]. Antibodies to ATP8b1 were generous gifts from D. Ortiz (Tufts University)[30] and M. Ananthanarayanan (Mount Sinai School of Medicine)[31]. This material is based upon work supported, in part, by the US Department of Veterans Affairs, Veterans Health Administration, Office of Research and Development, Biomedical Laboratory Research and Development. This work was supported by a Merit Review Award from the US Department of Veterans Affairs and US National Institutes of Health R01 grants HL068135, HL080229, HL081784, HL096376, HL097376 and HL098174 (to R.K.M.), HL70755, HL094488 and NIOSH OH008282 (to V.E.K.) and K23 HL075402 and U01 HL102288 (to L.D.). The contents do not represent the views of the Department of Veterans Affairs or the US government.

AUTHOR CONTRIBUTIONS

N.B.R. designed and executed cardiolipin-ATP8b1 binding, *in vitro* imaging and immunological studies and wrote the manuscript. L.D. edited the manuscript and conducted the human studies. B.B.C. performed *in vitro* (cardiolipin uptake, biochemical and molecular) experiments and all mouse studies. B.J.M. and M.D. contributed to human studies and statistical analyses. A.K.W., T.A.C., M.A., P.L.B., F.C.H. and S.N.M. assisted with *in vitro* studies. A.J.R. and C.P.O. assisted with mouse studies. D.M.M., E.C.H.-R. and C.A.E. conducted cardiolipin analysis. L.G. conducted surfactant studies. J.C.S. and G.M. designed and conducted *in vivo* imaging. V.E.K. designed and executed mass spectrometry of cardiolipin, with assistance from Y.Y.T., and provided editorial suggestions. R.K.M. revised the manuscript and directed the study.

COMPETING FINANCIAL INTERESTS

The authors declare no competing financial interests.

Published online at http://www.nature.com/naturemedicine/.
Reprints and permissions information is available online at http://npg.nature.com/reprintsandpermissions/.

1. Agency for Healthcare Research and Quality. Pneumonia most common reason for hospitalization. AHRQ News and Numbers, July 2, 2008. http://www.ahrq.gov/news/nn/nn070208.htm (2008).
2. Kadioglu, A., Weiser, J.N., Paton, J.C. & Andrew, P.W. The role of *Streptococcus pneumoniae* virulence factors in host respiratory colonization and disease. *Nat. Rev. Microbiol.* **6**, 288–301 (2008).
3. Rooney, S.A., Young, S.L. & Mendelson, C.R. Molecular and cellular processing of lung surfactant. *FASEB J.* **8**, 957–967 (1994).
4. Liau, D.F., Barrett, C.R., Bell, A.L., Cernansky, G. & Ryan, S.F. Diphosphatidylglycerol in experimental acute alveolar injury in the dog. *J. Lipid Res.* **25**, 678–683 (1984).
5. Ksenzenko, S.M. *et al.* Effect of triiodothyronine augmentation on rat lung surfactant phospholipids during sepsis. *J. Appl. Physiol.* **82**, 2020–2027 (1997).
6. Koppelman, C.M., Den Blaauwen, T., Duursma, M.C., Heeren, R.M. & Nanninga, N. *Escherichia coli* minicell membranes are enriched in cardiolipin. *J. Bacteriol.* **183**, 6144–6147 (2001).
7. Whitington, P.F., Freese, D.K., Alonso, E.M., Schwarzenberg, S.J. & Sharp, H.L. Clinical and biochemical findings in progressive familial intrahepatic cholestasis. *J. Pediatr. Gastroenterol. Nutr.* **18**, 134–141 (1994).
8. Bull, L.N. *et al.* A gene encoding a P-type ATPase mutated in two forms of hereditary cholestasis. *Nat. Genet.* **18**, 219–224 (1998).
9. Pawlikowska, L. *et al.* Differences in presentation and progression between severe FIC1 and BSEP deficiencies. *J. Hepatol.* **53**, 170–180 (2010).
10. Mizgerd, J.P. Acute lower respiratory tract infection. *N. Engl. J. Med.* **358**, 716–727 (2008).
11. Dullforce, P., Sutton, D.C. & Heath, A.W. Enhancement of T cell–independent immune responses *in vivo* by CD40 antibodies. *Nat. Med.* **4**, 88–91 (1998).
12. Grossmann, G. *et al.* Experimental neonatal respiratory failure induced by lysophosphatidylcholine: effect of surfactant treatment. *J. Appl. Physiol.* **86**, 633–640 (1999).
13. Paulusma, C.C. *et al.* Atp8b1 deficiency in mice reduces resistance of the canalicular membrane to hydrophobic bile salts and impairs bile salt transport. *Hepatology* **44**, 195–204 (2006).
14. Pawlikowska, L. *et al.* A mouse genetic model for familial cholestasis caused by ATP8B1 mutations reveals perturbed bile salt homeostasis but no impairment in bile secretion. *Hum. Mol. Genet.* **13**, 881–892 (2004).
15. Borron, P. *et al.* Surfactant-associated protein A inhibits LPS-induced cytokine and nitric oxide production *in vivo*. *Am. J. Physiol. Lung Cell. Mol. Physiol.* **278**, L840–L847 (2000).
16. Yamazoe, M. *et al.* Pulmonary surfactant protein D inhibits lipopolysaccharide (LPS)-induced inflammatory cell responses by altering LPS binding to its receptors. *J. Biol. Chem.* **283**, 35878–35888 (2008).
17. Kennedy, J.I. Jr. High alveolar surface tension pulmonary edema—relationship to adult respiratory distress syndrome. *J. Thorac. Cardiovasc. Surg.* **100**, 145–146 (1990).
18. Albert, R.K., Lakshminarayan, S., Hildebrandt, J., Kirk, W. & Butler, J. Increased surface tension favors pulmonary edema formation in anesthetized dogs' lungs. *J. Clin. Invest.* **63**, 1015–1018 (1979).
19. Sutrina, S.L. & Scocca, J.J. Phospholipids of Haemophilus influenzae Rd during exponential growth and following the development of competence for genetic transformation. *J. Gen. Microbiol.* **92**, 410–412 (1976).
20. Kagan, V.E. *et al.* Cytochrome c acts as a cardiolipin oxygenase required for release of proapoptotic factors. *Nat. Chem. Biol.* **1**, 223–232 (2005).
21. Sorice, M. *et al.* Cardiolipin on the surface of apoptotic cells as a possible trigger for antiphospholipids antibodies. *Clin. Exp. Immunol.* **122**, 277–284 (2000).

22. Wang, Z. & Notter, R.H. Additivity of protein and nonprotein inhibitors of lung surfactant activity. *Am. J. Respir. Crit. Care Med.* **158**, 28–35 (1998).
23. Ritov, V.B., Menshikova, E.V. & Kelley, D.E. Analysis of cardiolipin in human muscle biopsy. *J. Chromatogr. B Analyt. Technol. Biomed. Life Sci.* **831**, 63–71 (2006).
24. Benarafa, C., Priebe, G.P. & Remold-O'Donnell, E. The neutrophil serine protease inhibitor serpinb1 preserves lung defense functions in *Pseudomonas aeruginosa* infection. *J. Exp. Med.* **204**, 1901–1909 (2007).
25. McCormack, F.X., King, T.E. Jr., Voelker, D.R., Robinson, P.C. & Mason, R.J. Idiopathic pulmonary fibrosis. Abnormalities in the bronchoalveolar lavage content of surfactant protein A. *Am. Rev. Respir. Dis.* **144**, 160–166 (1991).
26. Hughes, D.A. & Haslam, P.L. Changes in phosphatidylglycerol in bronchoalveolar lavage fluids from patients with cryptogenic fibrosing alveolitis. *Chest* **95**, 82–89 (1989).
27. Jirsa, M. *et al.* Indel in the FIC1/ATP8B1 gene—a novel rare type of mutation associated with benign recurrent intrahepatic cholestasis. *Hepatol. Res.* **30**, 1–3 (2004).
28. van Mil, S.W., Klomp, L.W., Bull, L.N. & Houwen, R.H. FIC1 disease: a spectrum of intrahepatic cholestatic disorders. *Semin. Liver Dis.* **21**, 535–544 (2001).
29. Frick, A.G. *et al. Haemophilus influenzae* stimulates ICAM-1 expression on respiratory epithelial cells. *J. Immunol.* **164**, 4185–4196 (2000).
30. Ujhazy, P. *et al.* Familial intrahepatic cholestasis 1: studies of localization and function. *Hepatology* **34**, 768–775 (2001).
31. Frankenberg, T. *et al.* The membrane protein ATPase class I type 8B member 1 signals through protein kinase C ζ to activate the farnesoid X receptor. *Hepatology* **48**, 1896–1905 (2008).

ONLINE METHODS

Human samples. The study was approved by the University of Iowa and University of Pittsburgh Institutional Review Boards. After obtaining informed consent from the subjects, we collected tracheal aspirates with an inline suction catheter without saline dilution. Subjects were diagnosed with pneumonia (clinical diagnosis and confirmed with infiltrates on chest X-ray), CHF (clinical diagnosis and confirmed with pulmonary edema on chest X-ray). Control subjects were intubated for nonpulmonary illnesses (normal chest X-ray). Aliquots were sent for routine cultures.

Cells. MLE cells were cultured as previously described[32]. Cells were serum starved for 24 h and then exposed to 120 nmol ml^{-1} Infasurf (Forest Pharmaceuticals), phosphatidylcholine liposomes or cardiolipin (5–15 mol%) (Avanti Polar Lipids). Mouse alveolar type II cells, macrophages and fibroblasts were isolated as previously described[32]. Cell viability was determined with the CellTiter-Glo Luminescent Cell Viability assay (Promega). LDH release was assayed by monitoring the NAD-NADH reaction at a 340-nm wavelength.

[^{3}H]cardiolipin uptake. [^{3}H]cardiolipin (Moravek Biochemicals) was reconstituted in liposomes with Infasurf, added to medium and incubated for 2 h at 37 °C. Cellular uptake was terminated by washing with serum-free cold medium twice and 2% fatty acid–free BSA in PBS. Lipids were extracted (1 ml hexane: isopropanol (3:2, vol/vol)), solvents were dried and radioactivity (d.p.m.) in lipids was measured by scintillation counting.

Adenoviral expression. Full-length ATP8b1 was amplified from an expression clone in pcDNA3.1D/V5-His (Invitrogen) with forward and reverse primers with engineered EcoRI and SpeI restriction sites, respectively. The amplified product was directionally cloned into the EcoRI and BamHI sites of the adenovirus shuttle plasmid, pacAd5 CMV K-NpA provided by the University of Iowa Gene Transfer Vector Core that generated an adenoviral expression vector including V5-FL ATP8b1 (ref. 33).

Mice. C57BL/6 mice (Jackson Laboratories) and Atp8b1 mutant mice (a gift from L. Bull)[14] were used according to protocols approved by the University of Iowa and University of Pittsburgh Institutional Animal Care and Use Committees. Mice were infected i.t. with either *E. coli* (American Type Culture Collection 25922) (1×10^6 CFU) for 48 h or nontypable *H. influenzae* (2×10^8 CFU) or given agarose[29] for 72 h before lung lavage. For adenoviral gene transfer, mice received 2.5×10^8 plaque-forming units i.t. and 24 h later were given *E. coli* for 48 h. Mice were mechanically ventilated with a FlexiVent system[34]. Mice were also given *E. coli* and ventilated, and 48 h later diluent or ATP8b1 CBD peptide was delivered into lungs by a microsprayer aerosolizer. After 10 min, biophysical measurements were taken. For assay of lung edema, mice received cardiolipin (15 mM in 50 µl saline i.t.) or vehicle (50 µl saline). Evans Blue dye (40 µg per g body weight in 100 µl saline) was injected intravenously via the femoral vein 30 min later and BAL fluid was obtained. Dye concentration was determined with a spectrophotometer at a wavelength of 620 nm. For wet-dry weights, lungs were removed, blotted and placed in tared weigh boats and weighed. The lungs were then dried (24 h at 60 °C) and weighed again.

Fluorescent microscopy. Cells were plated (35-mm culture dishes) and incubated with NBD-cardiolipin and NBD-phosphatidylserine (25 °C), and then immediately incubated at 4 °C for 5 min before washing with medium. Fluorescence was detected by an epifluorescent microscope (Olympus).

Lentiviral stable cell line. Lentivirus expressing ATP8b1 was produced with pLenti6/V5-DEST by the University of Iowa Gene Transfer Vector Core. Cells were transduced with a final concentration of 4 µg ml^{-1} of polybrene (Sigma) in MEM-F12, at a multiplicity of transduction of 10:1. A final concentration of 2.5 µg ml^{-1} blasticidin (Invitrogen) was used to select for transduced cells.

Nitrobenzoxadiazole-lipid uptake. NBD-labeled phosphatidylserine (Avanti Polar Lipids) and NBD- cardiolipin (Invitrogen) were incubated with cells for 30 min at 37 °C. Lipids were extracted twice with 1 ml hexane:isopropanol (3:2, vol/vol). The solvents were evaporated under nitrogen, and lipids were dissolved in methanol. The fluorescence of NBD-labeled lipids was measured (excitation and emission at 460 nm and 530 nm, respectively) and quantified using standard curves for known amounts of the NBD-labeled lipids.

Nonyl acridine orange–cardiolipin quantification. Lipids were extracted[35,36], and cardiolipin bound to fluorescent nonyl acridine orange (NAO) was quantified with a spectrophotometer measuring NAO excitation and emission (494 nm and 530 nm) using standard curves[37]. Values were normalized for total phospholipid phosphorus[38] and expressed as ratios (mol%) of phosphorus (nmol) in cardiolipin to total phospholipid (nmol) within samples.

Lipid overlay. Lipid strips (Echelon Biosciences) were incubated with translation products in Tween 20, Tris-buffered saline solution with 1% fatty acid–free BSA. Strips were washed extensively, and radiolabeled protein was detected with V5-specific antibody (Invitrogen, R960-25) by immunoblotting.

ATP8b1 knockdown. A549 cells (American Type Culture Collection) were transfected twice with 2 µg of ATP8b1 ON TARGET plus SMARTpool siRNA or ON-TARGET plus Non-targeting Pool control siRNA (Dharmacon) for 48 h using Fugene 6 (Roche Diagnostics) before collection of the cells.

Statistical analyses. We used a Prism program version 4.03 (GraphPad) and ANOVA or Student's *t* test, with $P < 0.05$ indicative of significance. Kaplan-Meier survival estimates were done with SAS version 9.2 (SAS Institute). For human data, nonparametric testing with a Kruskal-Wallis and *post hoc* Wilcoxon rank-sum test was performed.

32. McCoy, D.M., Fisher, K., Ryan, A.J. & Mallampalli, R.K. Transcriptional regulation of lung cytidylyltransferase in developing transgenic mice. *Am. J. Respir. Cell Mol. Biol.* **35**, 394–402 (2006).
33. Chen, B.B. & Mallampalli, R.K. Calmodulin binds and stabilizes the regulatory enzyme, CTP: phosphocholine cytidylyltransferase. *J. Biol. Chem.* **282**, 33494–33506 (2007).
34. Zhou, J. *et al.* Adenoviral gene transfer of a mutant surfactant enzyme ameliorates *Pseudomonas*-induced lung injury. *Gene Ther.* **13**, 974–985 (2006).
35. Bligh, E.G. & Dyer, W.J. A rapid method of total lipid extraction and purification. *Can. J. Biochem. Physiol.* **37**, 911–917 (1959).
36. Folch, J., Lees, M. & Sloane Stanley, G.H. A simple method for the isolation and purification of total lipides from animal tissues. *J. Biol. Chem.* **226**, 497–509 (1957).
37. Kaewsuya, P., Danielson, N.D. & Ekhterae, D. Fluorescent determination of cardiolipin using 10-N-nonyl acridine orange. *Anal. Bioanal. Chem.* **387**, 2775–2782 (2007).
38. Mallampalli, R.K., Ryan, A.J., Salome, R.G. & Jackowski, S. Tumor necrosis factor-alpha inhibits expression of CTP:phosphocholine cytidylyltransferase. *J. Biol. Chem.* **275**, 9699–9708 (2000).

doi:10.1038/nm.2213